Direct Measurement of EGR Cooler Deposit Thermal Properties for Improved Understanding of Cooler Fouling

Michael J. Lance, C. Scott Sluder,
Hsin Wang and John M. E. Storey
Oak Ridge National Laboratory

ABSTRACT

Exhaust gas recirculation (EGR) cooler fouling has become a significant issue for compliance with NO_x emissions standards. This paper reports results of a study of fundamental aspects of EGR cooler fouling. An apparatus and procedure were developed to allow surrogate EGR cooler tubes to be exposed to diesel engine exhaust under controlled conditions. The resulting fouled tubes were removed and analyzed. Volatile and non-volatile deposit mass was measured for each tube. Thermal diffusivity of the deposited soot cake was measured by milling a window into the tube and using the Xenon flash lamp method. The heat capacity of the deposit was measured at temperatures up to 430°C and was slightly higher than graphite, presumably due to the presence of hydrocarbons. These measurements were combined to allow calculation of the deposit thermal conductivity, which was determined to be 0.041 W/mK, only ~1.5 times that of air and much lower than the 304 stainless steel tube (14.7 W/mK). The main determinant of the deposit thermal conductivity is density, which was measured to be just 2% that of the density of the primary soot particles (or 98% porous). The deposit layer thermal resistance was calculated and compared with estimates of the thermal resistance calculated from gas temperature data during the experiment. The deposit properties were also used to further analyze the temperature data collected during the experiment.

INTRODUCTION

Exhaust gas recirculation (EGR) has proven to be a useful means of reducing nitrogen oxides (NO_x) formation during the combustion process in compression-ignition engines for both conventional and low-temperature combustion modes. [1–5] Compact heat exchangers are now commonly installed to cool the EGR gases prior to mixing with the fresh air charge, further reducing NO_x formation. EGR coolers experience degradation of performance as a result of the buildup of particulate matter (PM) and unburned hydrocarbons (HC) in the gas-side flow paths of the cooler. These form a deposit layer that is less thermally conductive than the stainless steel of the tube enclosing the gas, resulting in lower heat exchanger effectiveness. [6–10] In the past, EGR coolers were sufficiently large and the NO_x targets sufficiently high that the cooler fouling process was of less importance. Now, smaller, more efficient coolers are beneficial from both a cost and a packaging standpoint. However, maintaining the EGR cooler at a high level of performance has become a significant issue in terms of achieving compliance with increasingly stringent NO_x regulations. [11–18]

There is little data in the literature to describe the thermal properties of EGR cooler deposits. Models of the fouling process and its effect on cooler performance require reasonably accurate data on the thermal properties of the layer and how they change with engine conditions and with time. Successful modeling of the fouling process represents the most efficient means of designing future EGR systems to reduce the impacts of fouling. To this end, deposits were formed in a

controlled manner on stainless steel tubes and the thermal conductivity was measured. We present here the experimental methodology and sources of error associated with measuring the thermal conductivity of soot cake.

The thermal conductivity (K) of materials is expressed by the equation:

$$K = \alpha \rho C_p$$

where is the thermal diffusivity, is the density and C_p is the specific heat. All three of these material properties must be measured in order to calculate the thermal conductivity from measured values. The difficulty arises from the fact that the microstructure of the EGR cooler deposit is extremely fragile and is deposited on hard stainless steel. If the deposit is disturbed during sample preparation, the density or thermal diffusivity may change which will greatly alter the calculated thermal conductivity.

EXPERIMENTAL METHODOLOGY

Studies of in-use EGR coolers can facilitate long-term evaluations of the fouling process, but because of their size and physical layout, full-size coolers are inconvenient for studies of the deposit layer properties. The extensive machining needed to extract a sample from a real cooler increases the risk of disturbance to the deposit. Furthermore, designs using round or internally-finned designs do not lend themselves to this study because measurement of thermal diffusivity by the flash method requires a flat surface so that heat transfer is unidirectional. Thus, a system was devised to utilize surrogate tubes to represent the EGR cooler for this study. Deposits were collected in these tubes and were subsequently analyzed to examine the deposit thermal properties.

ENGINE AND ENGINE OPERATING CONDITIONS – A 6.4-liter diesel V-8 engine from a model year 2008 Ford superduty pickup truck was used in this study. The engine served as an exhaust generator to supply engine exhaust to the surrogate tubes. The engine was operated at 2,150 RPM with a brake power output of 49 kW, consistent with a cruise condition. Experiments were carried out using ultra-low sulfur certification diesel (ULSD) sourced from Chevron-Phillips Specialty Chemical Company, a 5% volume blend of soy biodiesel in ULSD (B5), and a 20% volume blend of soy biodiesel in ULSD (B20). The soy biodiesel used for these blends was sourced from SoyGold, a BQ9000-certified supplier. Filter smoke number was measured at 1.5 using an AVL model 415S smoke meter; HC concentration was determined to be approximately 50 PPM using a California Analytical model 300M heated flame ionization detector. Use of B5 and B20 blends did not significantly change the operating parameters from those experienced with ULSD.

SURROGATE TUBES – The surrogate tubes used for this study were welded assemblies consisting of a 229-mm length of square-section 304 stainless steel tube with a 76-mm section of round 304 stainless steel tube (9.53-mm outer diameter and 0.71-mm wall thickness) welded to each end. The round sections were needed to facilitate gas- and water-side seals for the surrogate tubes. The square-section tubing was 6.35 mm x 6.35 mm with a wall thickness of 0.51 mm. The tubes were individually surrounded by a simple shell-type water jacket fabricated using Swagelok® fittings and removable ferrules. The square-section tubing was selected for two reasons. A flat surface wall was required for flash-method thermal diffusivity measurements of the deposit layer, and a simple tube geometry was desired to enhance the value of the results to the modeling community.

SURROGATE TUBE CONDITIONS – Four surrogate tubes were simultaneously exposed to exhaust conditions for each experiment in this study. The tube gas inlets were manifolded together and connected to the engine exhaust manifold upstream of the turbine inlet. The exhaust gas flow rate through each tube was individually controlled to a nominal 31 standard liters-per-minute (SLPM) rate. The coolant flow rate was maintained at or above 1 liter per minute of water per surrogate tube. The engine conditions outlined previously produced tube inlet temperatures of ~375°C.

Two sets of experiments were performed for each of three fuels (ULSD, B5, B20). Extensive results from these studies have been previously reported. (10) One surrogate tube was collected from each fuel to begin studies of the deposit thermal properties. Each tube was exposed to engine exhaust as outlined above for 12 hours with a coolant temperature of 90 °C.

Each tube was broken down to produce the necessary samples. Samples were made by milling the wall thickness down to ~100 µm which allowed the metal substrate to be broken without disturbing the soot cake. Each tube produced 4 25-mm long samples for density measurement, one 50-mm long sample for thermal diffusivity measurement and two 13-mm long samples for microstructural analysis as well as loose soot powder for specific heat measurements.

RESULTS

SPECIFIC HEAT –The specific heat of the soot powder was measured using a Stanton-Redcroft Differential Scanning Calorimeter (DSC) with the soot in an open

pan in argon up to 430°C using sapphire as a reference. Since the heat capacity is independent of the density of the soot cake, the soot collected from the tubes was pressed into pellets to increase the mass being heated. Two runs were performed on each sample so as to release water and hydrocarbons in the first run and to collect heat capacity data on the partially devolatilized soot in the second run. A closed pan would have prevented mass loss from evaporation of water and devolatilization of hydrocarbons but would have introduced errors due to the enthalpies associated with these transitions. By using an open pan, the heat capacity measured in the second run was truly unperturbed by any heat produced or absorbed by the evaporation of water or the oxidation of hydrocarbons, respectively.

Figure 1 shows the specific heat capacity from 25°C up to 430°C for soot from ULSD fuel. The first run (dashed line) devolatilized the sample and can not be used for C_p. The peak around 100°C is from the endothermic evaporation of water which increases the heat capacity since the material absorbs heat. The peak that starts around 250°C is exothermic and so is likely due to the oxidation of volatile hydrocarbons. Since we only heat to 430°C, this reaction is only partially completed so some hydrocarbons are still present in the sample for the second run. The cooling curve from the first run is lower than the second run (solid lines) because the mass of the sample has decreased after heating and so the initial weight used for calculating C_p is too high which forces C_p down.

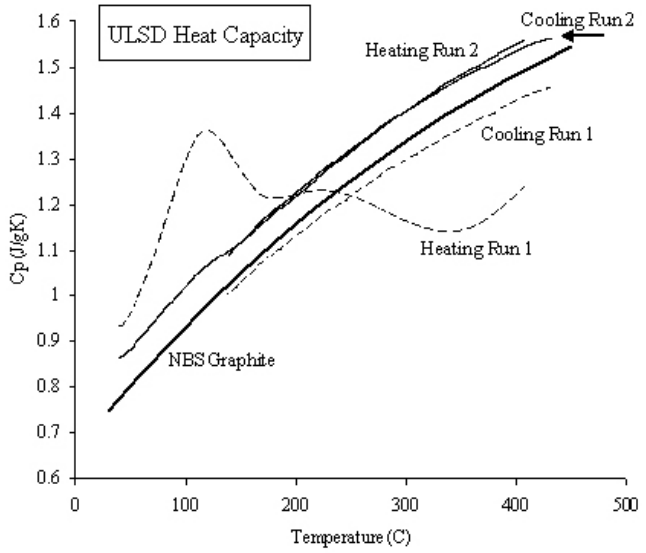

Figure 1. Specific heat capacity for tube deposit material derived from operation with ULSD.

The second run (solid line) had higher C_p than a standard National Bureau of Standards (NBS) graphite data. This difference is likely due to the presence of hydrocarbons that have not been completely removed from the soot. Since hydrocarbons have a lower molecular weight than just carbon, the heat capacity will be higher which may result in higher C_p measured here. Between runs, the sample is re-weighed and picks up some water which produces a small water endotherm during the second run. Heating and cooling traces for the second run were very similar to each other for all samples which show that the samples were fairly dry after the first run.

Figure 2 shows the heat capacity for all fuels and a standard Printex soot powder as well as the NBS graphite reference data for the heating segment of the second run. Heat capacity of all samples is higher than pure graphite measured by the National Bureau of Standards. Again, this shows that the hydrocarbons will tend to increase the C_p of the soot and hence the thermal conductivity.

Printex is identical to NBS graphite (within experimental error and ignoring adsorbed water) which shows that it has no volatiles (hydrocarbons) present. It is likely that if the samples were heated to 700°C in the first run, all of the data from the second run would fall on top of the NBS graphite and Printex curves since there would be no hydrocarbons present. Nevertheless, the presence of hydrocarbon increases the C_p less than 6% over Printex and graphite for all the soot samples so it is not expected to be a large source of error. More importantly, the variations in the heat capacity of the soot, irrespective of the source, will not greatly alter the calculated value of thermal conductivity of the deposit material. Resulting value of specific heat capacity (at 25 °C) for ULSD, B5, and B20 deposits were 0.8668, 0.8170, and 0.8706 J/gK, respectively.

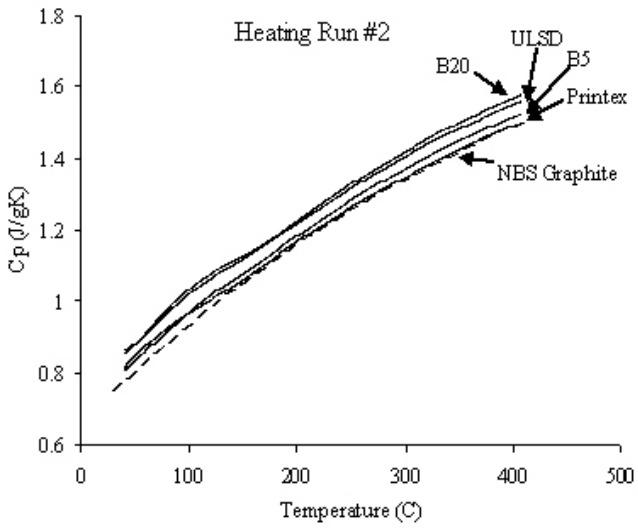

Figure 2. Specific heat capacity data for deposit material derived from use of B5 and B20 blends.

DENSITY – As described above, 25-mm long sections of tube with attached deposits were used to measure density. Since the length and the cross-sectional area of the tube were known, all that was required to measure the volume of the deposit was the thickness of the deposit. A number of methods were attempted including laser profilometry, epoxy-mounting a cross-section and focusing on the metal and soot surfaces to measure the height with an optical microscope. The best method was to simply look at the pristine deposit layer in cross section after breaking the metal (following milling). This method ensured that the deposit microstructure was completely undisturbed. Figure 3 shows the cross-section of the ULSD deposit to be ~0.41 mm thick. The mass of the soot in each 25-mm long segment of tube was measured by subtracting the soot loaded segment from the same segment after being cleaned.

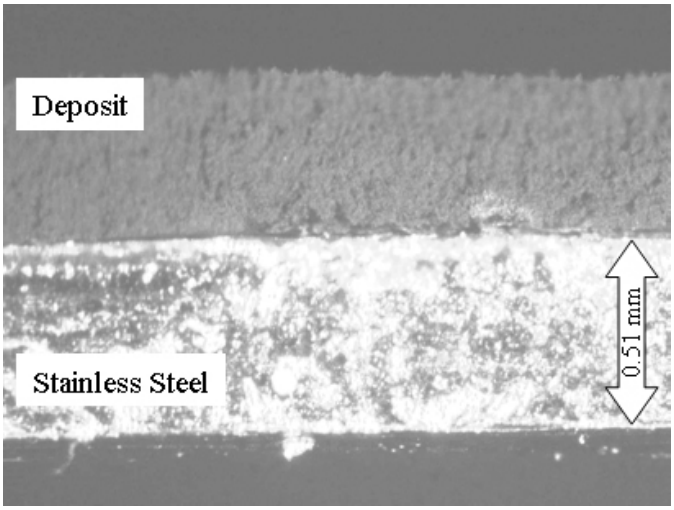

Figure 3. Micrograph showing deposit layer attached to the stainless steel tube wall.

Deposit thickness for the ULSD, B5, and B20 deposits was measured to be 0.4140, 0.3725, and 0.3600 mm, respectively. The resulting densities of the deposits were calculated to be 0.0316, 0.0363, and 0.0379 g/cm^3, respectively. The average density of all three deposit samples was calculated to be 0.035 g/cm^3 which results in a porosity of 98% using a primary soot particle density of 1.77 g/cm^3. (19)

The deposit density was measured on nascent samples that had not been through a devolatilization step. From the heat capacity results, it is expected that ~10% of the nascent deposit mass was composed of water and hydrocarbons. Removal of this material from the soot will therefore reduce the mass of the sample. It is unclear from the data gathered to date what impact this would have on the deposit density. Significant morphological changes were observed in samples that were left in open air for a few weeks. The underlying reasons for this behavior are unclear, but the authors surmise that gain or loss of water from the air may be causing a deposit density change over time. It should also be stated that very large amounts of water and hydrocarbon caused by condensation in actual EGR systems may have the effect of collapsing the fragile porous deposit structure thereby dramatically increasing the density. In either case, one could reasonably expect a significant change in the calculated thermal conductivity as a result of the deposit density change.

THERMAL DIFFUSIVITY – A 50-mm long window was milled out of the center of each tube so as to provide access for thermal diffusivity measurements using the flash technique (ASTM E1461). In this procedure, the deposit surface on the inside of the tube is exposed to a short pulse of heat generated by a Xenon flash lamp and the temperature change is measured on the back metal surface of the tube with an infrared (IR) detector as a function of time. Figure 4 shows the voltage output of the IR detector as a function of time for a stainless steel tube with no deposit and a tube with a deposit resulting from operation with B20. The voltage is proportional to the temperature of the deposit surface which likely increases only a few degrees due to the flash lamp.

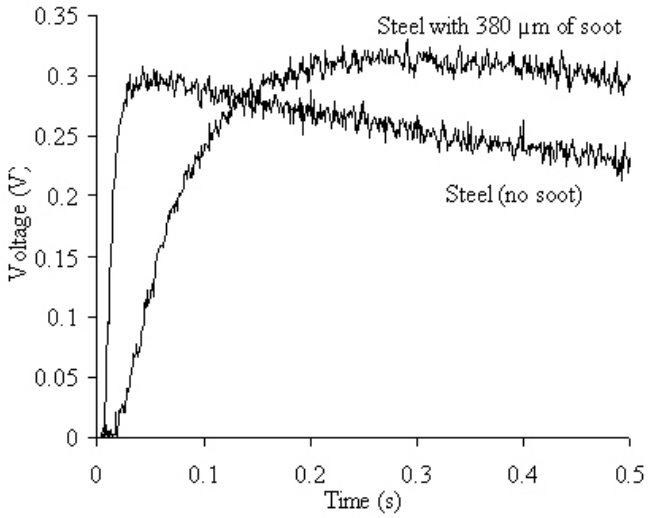

Figure 4. Example data from the flash-technique for thermal diffusivity.

The presence of the deposit increases the time required for the deposit surface to reach a maximum temperature on the detector side of the sample. The magnitude of the detector response is arbitrary; it is the time required to achieve half the maximum value that is used to determine thermal diffusivity for the sample. Five measurements were made on each tube. The measured increase in detector voltage vs. time is fitted with a curve that assumes ideal one-directional heat flow and produces a parameter called 'average loss'. This is a measurement of how far the sample deviates from the ideal heat transfer curve and which allowed for the elimination of spurious data points. Since the diffusivity

of the metal substrate and the deposit are measured in aggregate, an iterative approach was necessary to extract the thermal diffusivity of the deposit from the metal/deposit composite value. The ULSD, B5, and B20 deposits exhibited thermal diffusivities of 0.0190, 0.0110, and 0.0093 cm^2/s, respectively. The average value for all three samples was 0.013 cm^2/s. From the literature, the stainless steel tube wall was assumed to have a thermal diffusivity of 0.0395 cm^2/s. (20)

THERMAL CONDUCTIVITY – The thermal conductivities were calculated for each sample from the measurements outlined above. The resulting values for ULSD, B5, and B20 were 0.057, 0.034, and 0.032 W/mK, respectively with the average being 0.041 W/mK. The extremely high porosity is the main determinant of the thermal conduction properties of the deposit since it is mostly composed of air. Air has a very low thermal conductivity (0.025 W/mK) compared to dense graphite (~10 W/mK).

The average thermal conductivity of the deposit is only slightly above that of air and is much lower than that of 304 stainless steel (14.7 W/mK). Given the porosity of the soot cake at ~98%, and a thermal conductivity of the graphite particles of 5 W/mK, the calculated thermal conductivity would be ~0.1 W/mK assuming a linear rule of mixtures which compares well to our measurement. Several types of insulating materials (such as glass fiber and R-12 expanded and extruded polystyrene) exhibit thermal conductivities comparable to that described here for the deposit layer. (20) The largest property difference between the soot and the steel substrate is the density of the deposit; hence it is most responsible for the relatively low values of deposit thermal conductivity.

EFFECTS OF ADSORBED SPECIES – The potential clearly exists for adsorbed species (water and hydrocarbons) to influence the thermal properties of the deposits. Examination of the data in figure 1 for the first heating run shows that the presence of water and hydrocarbons significantly changes the measured specific heat of the deposit. This results from the required heat of vaporization of the volatile material. While it would be inappropriate to characterize this effect as a real specific heat value change, in real systems the phase changes would occur in transient conditions and lead to an apparent change in the thermal resistance posed by the deposit layer in the EGR cooler. Furthermore, the presence of adsorbed water and hydrocarbons could conceivably lead to densification of the layer, reducing the void volume and increasing the overall thermal conductivity even in the absence of phase-change processes.

A companion study that has been previously reported showed evidence that the thermal properties of the deposit layer were not constant. (10) The tube samples analyzed for this study were generated at the 12-hour exposure time for which data are shown in the previous study. These samples had relatively low (~6%) volatile content compared with other samples that had up to 25% volatile content. All of these samples were gathered at a very low hydrocarbon level. Taken together, the data from the previous study and those reported here suggest strongly that adsorbed species play a strong role in determining the overall thermal properties of the deposit. Studies are planned for higher hydrocarbon conditions and are expected to provide additional understanding of the relationship between thermal properties and adsorbed species in deposits.

CONCLUSIONS

- A methodology for collecting deposits in surrogate EGR cooler tubes has been demonstrated.
- Measurements of the thermal properties of the deposit layer have been successfully accomplished.
- Average results for a limited number of samples has shown that the thermal conductivity of EGR cooler deposits with low levels of condensed HCs are quite low; measured values average 0.041 W/mK. This result is comparable to the thermal conductivity of materials known as effective insulators.
- More studies are needed to characterize the range of variation in deposit thermal properties that can be expected in practice and to lend understanding to the connections between operational conditions and the resulting property variations.

ACKNOWLEDGMENTS

The authors gratefully acknowledge the funding support of Kevin Stork, Dennis Smith, and Steve Goguen of the United States Department of Energy, Office of Vehicle Technologies. We would also like to thank Dan Styles of Ford Motor Company for providing the engine and funding the development of the sampling system and methodology that was used in this study. We also would like to thank Dr. Wally Porter for the specific heat measurements.

DISCLAIMER

REFERENCES

1. Dickey, D. W., Ryan, T., and Matheaus, A. C., "NO_x Control in Heavy-Duty Diesel Engines—What is the limit?" SAE Paper Number 980174, SAE International, 1998.
2. Ishikawa, N., Ohkubo, Y., and Kudou, K., "Study on the Effects of EGR Cooler Performance on Combustion Properties of the Pre-Mixed Compression Ignition Combustion by Multi Cylinder DI Diesel Engine," SAE Paper 2007-01-1881, SAE International, 2007.
3. Pickett, L. M., and Siebers, D. L., "Non-Sooting, Low Flame Temperature Mixing-Controlled DI Diesel Combustion," SAE Paper Number 2004-01-1399, SAE International, 2004.
4. Idicheria, C. A., and Pickett, L. M., "Soot Formation in Diesel Combustion under High-EGR Conditions," SAE Paper Number 2005-01-3834, SAE International, 2005.
5. Sluder, C. S., and Wagner, R. M., "An Estimate of Diesel High-Efficiency Clean Combustion Impacts on FTP-75 Aftertreatment Requirements," SAE Paper Number 2006-01-3311, SAE International, 2006.
6. Lepperhoff, G., and Houben, M., "Mechanisms of Deposit Formation in Internal Combustion Engines and Heat Exchangers," SAE Paper Number 931032, Society of Automotive Engineers, 1993.
7. Zhang, R., Charles, F., Ewing, D., Chang, J. S., and Cotton, J. S., "Effect of Diesel Soot Deposition on the Performance of Exhaust Gas Recirculation Cooling Devices," SAE Paper Number 2004-01-0122, SAE International, 2004.
8. Hoard, J. W., Abarham, M., Styles, D., Giuliano, J. M., Sluder, C. S., and Storey, J. M. E., "Diesel EGR Cooler Fouling," SAE Paper Number 2008-01-2475, SAE International, 2008.
9. Sluder, C. S., Storey, J. M. E., Styles, D., Giuliano, J., and Hoard, J. W., "Hydrocarbons and Particulate Matter in EGR Cooler Deposits: Effects of Gas Flow Rate, Coolant Temperature, and Oxidation Catalyst," SAE Paper Number 2008-01-2467, SAE International, 2008.
10. Sluder, C. S. and Storey, J. M. E., "EGR Cooler Performance and Degradation: Effects of Biodiesel Blends," SAE Paper Number 2008-01-2473, SAE International, 2008.
11. Bravo, Y., Lazaro, J. L., and Garcia-Bernad, J., "Study of Fouling Phenomena on EGR Coolers due to Soot Deposits: Development of a Representative Test Method," SAE Paper Number 2005-01-1143, SAE International, 2005.
12. Bravo, Y., Moreno, F., and Longo, O., "Improved Characterization of Fouling in Cooled EGR Systems," SAE Paper Number 2007-01-1257, SAE International, 2007.
13. Grillot, J. M., and Icart, G., "Fouling of a Cylindrical Probe and a Finned Tube Bundle in a Diesel Exhaust Environment," *Experimental Thermal and Fluid Science 1997,* 14:442–454. Elsevier Science, Inc., 1997.
14. Ismail, B., Charles, F., Ewing, D., Cotton, J. S., and Chang, J-S, "Mitigation of the Diesel Soot Deposition Effect on the Exhaust Gas Recirculation (EGR) Cooling Devices for Diesel Engines, SAE Paper Number 2005-01-0656, SAE International, 2005.
15. Ismail, B., Ewing, D., Cotton, J. S., and Chang, J-S., "Characterization of the Soot Deposition Profiles in Diesel Engine Exhaust Gas Recirculation (EGR) Cooling Devices using a Digital Neutron Radiography Imaging Technique," SAE Paper Number 2004-01-1433, SAE International, 2004.
16. Charles, F., Ewing, D., Becard, J., Chang, J-S., and Cotton, J. S., "Optimization of the Exhaust Mass Flow Rate and Coolant Temperature for Exhaust Gas Recirculation (EGR) Cooling Devices Used in Diesel Engines," SAE Paper Number 2005-01-0654, SAE International, 2005.
17. Usui, S., Ito, K., and Kato, K., "The Effect of Semi-Circular Micro Riblets on the Deposition of Diesel Exhaust Particulate," SAE Paper Number 2004-01-0969, SAE International, 2004.
18. Castano, C., Sanchez, A., Grande, J. A., and Paz, C., "Advantages in the EGR Cooler Performance by Using Internal Corrugated Tubes Technology," SAE Paper Number 2007-26-019, SAE International, 2007.
19. K. Park, D. B. Kittelson, M. R. Zachariah and P. H. McMurry, "Measurement of inherent material density of nanoparticle agglomerates," *Journal of Nanoparticle Research* **6** 267–272 (2004).
20. Frank P. Incropera and David P. Dewitt, Fundamentals of Heat and Mass Transfer, 3rd Edition. John Wiley & Sons, 1990.

CONTACT

Michael J. Lance, lancem@ornl.gov